Egyptian Journal of Chemistry

http://ejchem.journals.ekb.eg/

Corrosion Behavior of Ni And Ni-Base Alloy in Acidic Solutions

Lamiaa Z. Mohamed

Mining, Petroleum, and Metallurgical Engineering Department, Faculty of Engineering,

Cairo University, Egypt.

Abstract

The corrosion behavior of pure Ni and 65Ni-24Cr-10Mo alloy in HCl and H_2SO_4 solutions were investigated using weight-loss and electrochemical methods. The effects of temperature and acidic media were studied to define the main differences in the corrosion behavior of these materials. The results of both techniques revealed lower values of corrosion rates for the 65Ni-24Cr-10Mo alloy compared to pure Ni. Generally, the corrosion rates for both materials increase with increasing temperature in both acids with higher rates in HCl compared to H_2SO_4 at all conditions. Results of weight-loss and potentiodynamic tests were in a good agreement and indicated that the alloy 65Ni-24Cr-10Mo is a high resistance to corrosion in HCl and H_2SO_4 acidic solutions than pure Ni. The activation energies (Ea) of the dissolution process of Ni and alloy have calculated. The activation energy of Ni in HCl is 18 kJ/mole and in H_2SO_4 is 20 kJ/mole where for the alloy in HCl is 18 kJ/mole and in H_2SO_4 is 32 kJ/mole.

Keywords: Pure Ni; Ni-based alloy; Corrosion rate; Acidic solution; Microstructures

1. Introduction

The corrosion process can be described by interaction between the metal surface and the environment as the deterioration of metallic materials [1, 2]. Ni and Ni alloys have many industrial applications and used in highly aggressive environments [3, 4]. The acidic solutions are widely used in manufacturing processes such as plating, electro-winning and pickling processes. Ni-base alloys have been used in heat exchangers and various components of water pressurized reactors. This is because they have a strong passive film on the metal surface which gives excellent corrosion resistance in a wide range of corrosive media [5, 6]. The stability of this passive film is impaired and pitting corrosion occurs when these alloys are polarized in environments containing certain aggressive ions such as chloride over certain electrode potentials [5]. Alloying elements can be added to Ni alloys to produce a wide variety of alloys such as Cr and Mo

which give the alloys a high corrosion resistance [7-10]. If the Cr is sufficient enough, the Cr_2O_3 passive oxide layer is grown on the surface [11]. The use of Ni alloys as structural materials depends highly on the concentration and the proportion of alloying components, in particular Cr and Mo [12, 13]. The Cr and Mo in Ni- alloys hinder the effective breakdown of the Ni matrix, though Cr ensures its passivity, and Mo impedes it. The properties of the medium specify a minimum Cr content necessary to passivity and increase with increase in corrosiveness. The Ni alloys with up to 20% Cr are the basis for some refractory and heat-resistant alloys [12]. Special interest is given to alloys of the Ni-Cr-Mo system, which is commonly used in very aggressive media such as hydrochloric (HCl) and sulfuric (H2SO4) acids. This research assesses the role of the alloying elements of the 65Ni-24Cr-10Mo alloy than of pure Ni in the corrosion behavior in HCl and H_2SO_4 solutions using a weight-

_____

loss and potentiodynamic polarization method. The corroded surfaces of pure Ni and 65Ni-24Cr-10Mo alloy after being immersed in 1M HCl solutions for 96

hr were examined using a scanning electron microscope (SEM) and energy dispersive x-ray analysis (EDAX).

2. Experimental work

2.1 Materials and Solutions

The chemical compositions of the two materials used in the investigation are pure Ni (99.9% Ni) and Ni-based alloy (65% Ni-24% Cr-10% Mo). These alloys have a cylindrical sample shape that was ground with emery papers 320, 400, 800, 1000 and 1200 grade then polished by 0.3 µm alumina paste. The polishing of all the surfaces of the specimen was done. Use dual

2.2 Apparatus and Experimental Procedure

During the experiments on weight-loss, pure Ni and 65Ni-24Cr-10Mo alloy were weighed a cylindrical shape sample (w_1) and suspended in 100 ml beaker respectively in 1 M solutions of specific acids. After 30, 60, 90, 120, 150 and 200 min the samples were recovered, washed with distilled H_2O, dried with acetone and reweighed (w_2). The immersion time was accepted as the optimal immersion time with a slightly higher weight-loss. From the weight-loss data, the corrosion rate of pure Ni and the 65Ni-24Cr-10Mo alloy was calculated using Eqs. 1 and 2 [14]:

$$\Delta W = W_1 - W_2 \qquad (1)$$

$$C.R. \ (mg/cm^2.h) = \frac{weight \ loss}{Area \ x \ time} \qquad (2)$$

Where w_1 and w_2 are the weight of samples before and after immersion in the corrosive medium respectively. The prepared weighted pure Ni and 65Ni-24Cr-10Mo alloy samples were immersed in 1 M concentration of

2.2.3. Surface Morphology

The scanning electron microscope (SEM) images were obtained by using SEM Model Quanta 250 FEG (Field Emission Gun) attached with Energy Dispersive X-ray Analyses unit (EDAX), with

distilled H_2O, a stock solution of analytical grade HCl acid (37%, 1.18 g/L) and H_2SO_4 acid (98%, 1.84 g/L) were collected. Acid solutions with appropriate concentrations of 1 M were prepared by suitable dilutions. All the chemicals used in the current investigation were of analytical grade in the preparation of solutions.

2.2.1 Weight-loss

corroding at 30 ° C, 40 ° C and 60 ° C for 3 hr to study the effect of temperature. It took the final weight; it measured the weight-loss and corrosion rate.

2.2.2 Potentiodynamic polarization

The electrochemical experiments were carried out using the Voltalab 40 Potentiostat PGZ301 made in Germany. Potentiodynamic polarization studies were performed with the test specimens in the range from -0.4 V to +0.4 V using a scan rate of 5 mV/sec. The corrosion rate, C.R., can be computed using Faraday's Law as follows [9, 15]:

$$C.R. \ (\mu m/year) = 3.3 \, I_{corr} \, \frac{M}{zd} \qquad (3)$$

Where; z = ionic charge, M = atomic weight of Ni-alloy, d = density of Ni-alloy, and I_{corr} = corrosion current density, $\mu A/cm^2$.
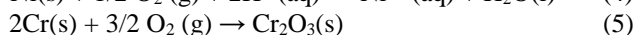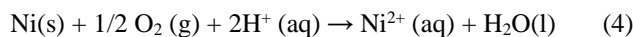
accelerating voltage 30. SEM and EDAX analyses were used to define the morphology of surface attack and the chemical composition of corrosion products on pure Ni and 65Ni-24Cr-10Mo alloy After 96 hr of immersion in 1 M HCl solution

3. Results and Discussion

3.1. *Weight-loss measurements*

The weight-loss calculation was described as ideally good as other alloy corrosion assessment techniques [16]. The weight-loss method was used in this investigation to evaluate the corrosion feature of pure Ni and 65Ni-24Cr-10Mo alloy in acidic HCl and H_2SO_4 solution. The weight-loss of each of the two samples was reported before immersion and measured

_____

at different temperatures to obtain the weight-loss after 3 hr of total immersion in the medium. Corrosion of the metal surface in its initial stage is a heterogeneous chemical reaction. The experimental results classify Ni de-alloy and Cr oxidation as dominant corrosion reactions in the high subcritical temperature range as follows [17]:

$$Ni(s) + 1/2\ O_2\ (g) + 2H^+\ (aq) \rightarrow Ni^{2+}\ (aq) + H_2O(l) \qquad (4)$$
$$2Cr(s) + 3/2\ O_2\ (g) \rightarrow Cr_2O_3(s) \qquad\qquad\qquad (5)$$

The corrosion rate of pure Ni and 65Ni-24Cr-10Mo alloy exposed to the acidic solution at 3 hr was calculated by the weight-loss method at 30 ° C to 60 ° C as seen in Fig.1. The weight-loss and corrosion rate increased in HCl and H_2SO_4 solution for two samples by increasing the temperature to 60 °C. The increasing temperature usually increases the solubility of protective films by increasing the constituent particle's average kinetic energy. As the average kinetic energy increases, the particles move more quickly and collide more often, increasing in the reaction rate [18, 19]. The increase in weight-loss may also be due to reactant diffusion and ionization or an increase in protective layer solubility, which makes the surface susceptible to corrosion [14].
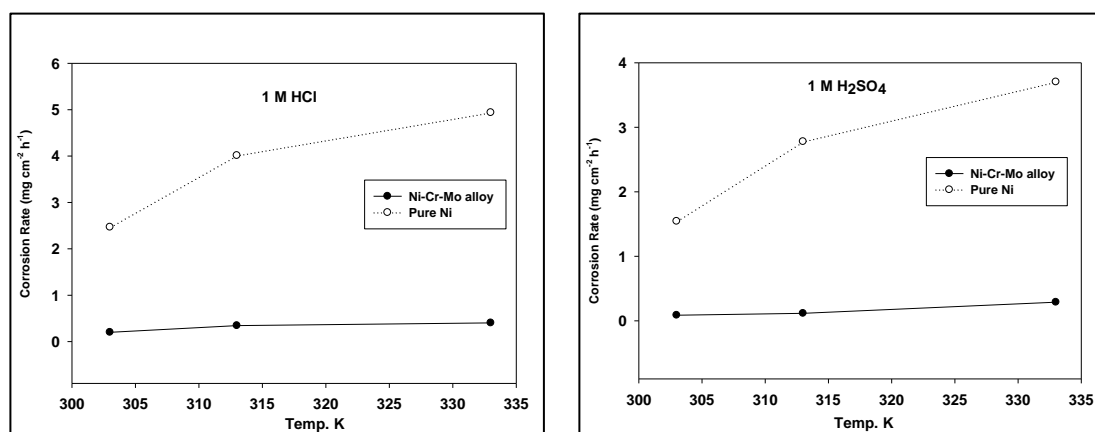

Fig. 1. Corrosion rates of pure Ni and 65Ni-24Cr-10Mo alloy exposed to different acids by weight-loss method.

Fig. 1. Proves that the corrosion rate increased due to the formation of the nickel hydroxide layer in the initial with an increase in acid and temperature. As the concentration increases, the nickel hydroxide protective layer on the pure Ni surface is formed, which reduces the weight-loss [14]. The 65Ni-24Cr-10Mo alloy's corrosion rate in various acid mediums decreases as compared to pure Ni due to the existence of Mo. Because of its residual tolerance, the 65Ni-24Cr-10Mo alloy was the best choice, although they are limited in temperature at higher acid concentrations. The significant discoveries are the excellent 65Ni-24Cr-10Mo alloy corrosion resistance in H_2SO_4 solution.

Temperature investigations are important in corrosion studies as they allow the determination of the activation energy (E_a) and the dissolution process to be calculated [20]. The apparent activation energies (E_a) were measured from Arrhenius Eq. 6 [21] and the results are presented in Table 1.

$$\ln C.R. = \ln A - \frac{E_a}{RT} \qquad (6)$$

Where A is a constant, R is the 8.314 J/mol.K universal gas constant, and T is the absolute temperature (K). The ln (C.R.) vs. absolute temperature (1/T) reciprocal plot as shown in Fig. 2. It provides a straight line with slope= $- E_a / R$ from which the values of the activation energy for the corrosion process are measured and tabulated in Table 1. The enthalpy of activation and entropy of activation were determined using transition state Eq. 7 [22, 23].

$$\ln \left(\frac{C.R}{T}\right) = \ln \left(\frac{R}{Nh}\right) + \frac{\Delta S_{ads}}{R} - \frac{\Delta H_{ads}}{RT} \qquad (7)$$

Where h is Plank's constant and N is Avogadro's number. A plot of ln (CR/T) vs. 1/T which illustrates in Fig. 3. exists a straight show with slope = $-\Delta H_{ands}$ /R and intercept = ln(R/Nh) + ΔS_{ads} /R. The calculated values of enthalpy and entropy from the plots are presented in Table 1. The E_a values of H_2SO_4 acid are greater than 20 kJ/mol; this suggested that the whole process is controlled by surface reaction [24]. The ΔS values are large and negative; this means that the activated complex in the rate determination phase reflects association rather than dissociation implying a decrease in disorder occurring. The positive signs of ΔH reflect that transition state (the activated complex) is an endothermic process.

Table 1. The values of activation parameters of pure Ni and 65Ni-24Cr-10Mo alloy in different acids from corrosion rate values of weight-loss method

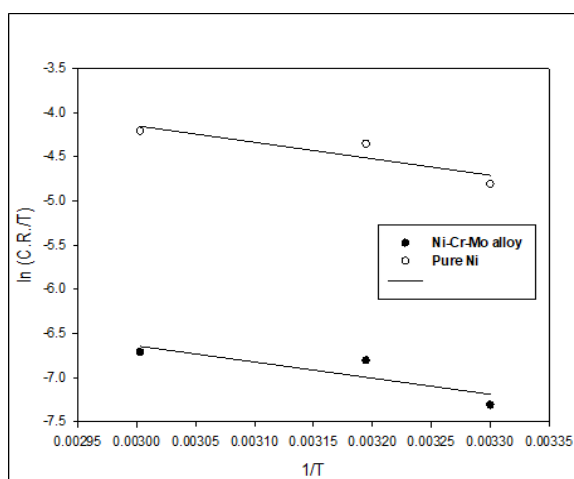| Samples	HCl			H$_2$SO$_4$		
	E$_a$ kJ/mole	ΔH kJ/mole	ΔS J/(mole.K)	E$_a$ kJ/mole	ΔH kJ/mole	ΔS J/(mole.K)
Pure Ni	18.120	15.474	-185.62	23.025	20.381	-173.21
65Ni-24Cr-10Mo alloy	17.843	15.196	-207.17	34.428	31.784	-160.97
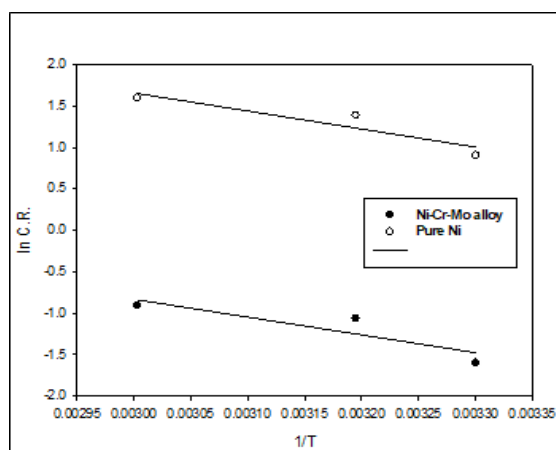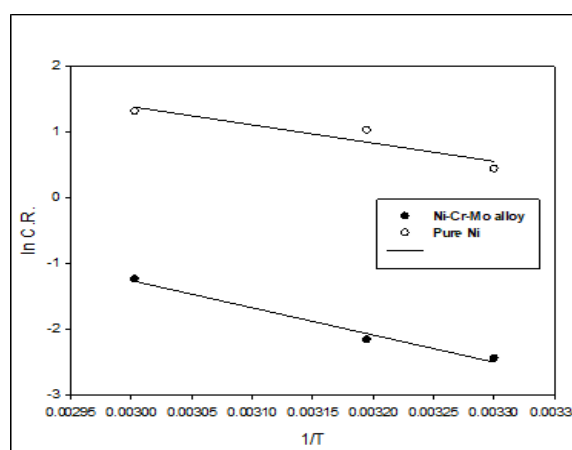
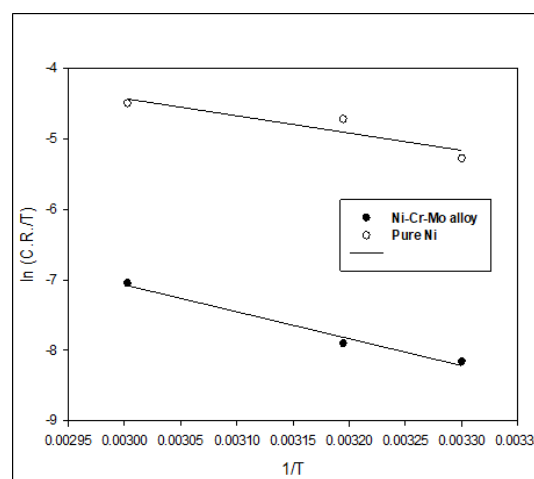(a)   (b)

Fig. 2. Arrhenius plots of ln C.R. vs. 1/T for pure Ni and 65Ni-24Cr-10Mo alloy exposed to different acids by weight-loss method (a) 1 M HCl and (b) 1M H$_2$SO$_4$

(a)   (b)

Fig. 3. Plots of ln (C.R./ T) versus 1/T for pure Ni and 65Ni-24Cr-10Mo alloy exposed to acids by weight-loss parameter (a) 1 M HCl and (b) 1M H$_2$SO$_4$

3.2. Potentiodynamic Polarization

The anodic polarization curves in Fig. 4 are typical of active material for pure Ni and active–passive transition in the 65Ni-24Cr-10Mo alloy in different acidic media. The cathodic current is due to the evolution of hydrogen gas, according to the following reaction [5]:

$$2H+ + 2e^- \rightarrow H_2 \quad (8)$$
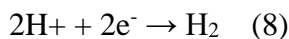
The electrochemical parameters such as corrosion potential, E_{corr}, corrosion current density, I_{corr}, and corrosion rate, C.R., are tabulated in Table 2. It was found that increasing the temperature from 30 °C to 60 °C leads to increasing the corrosion current density, I_{corr}, corrosion rate, C.R., accompanied by an almost change in the corrosion potential, E_{corr}, of the two samples. The shift of potential in the less negative direction came from the thin layer formation of corrosion products that partially decreases the attack on the alloy surface by an obstruction in a number of its exposed areas. The potential difference between the two samples is probably due to the higher ability of the 65Ni-24Cr-10Mo alloy in developing a thicker layer of corrosion products, which retains a higher corrosion resistance compared to pure Ni. In 1 M HCl solution, the high temperature produces more severe corrosion about 17.255 µm/y for pure Ni.

Table 2. Electrochemical parameters of pure Ni and 65Ni-24Cr-10Mo alloy in different acids media at different temperature by potentiodynamic polarization method

| Samples	Temp., °C	1 M HCl				
		E_{corr} V	I_{corr} µA/cm^2	C.R. µm/y	βa, V/dec	βc, V/dec
Pure Ni	30	-0.253	0.079	0.8649	0.13	0.11
	40	-0.309	0.794	8.649	0.11	0.11
	60	-0.303	1.584	17.255	0.20	0.06
65Ni-24Cr-10Mo alloy	30	-0.144	0.025	0.297	0.25	- 0.16
	40	-0.147	0.158	1.879	0.50	-0.13
	60	-0.189	0.398	4.734	0.25	-0.10
Samples	Temp., °C	1 M H$_2$SO$_4$				
		E_{corr} V	I_{corr} µA/cm^2	C.R. µm/y	βa, V/dec	βc, V/dec
Pure Ni	30	-0.292	0.039	0.4248	0.20	-0.10
	40	-0.243	0.1348	1.4684	0.60	-0.02
	60	-0.292	0.149	1.6231	0.40	-0.18
65Ni-24Cr-10Mo alloy	30	0.196	0.0072	0.0856	0.40	0.14
	40	-0.034	0.0316	0.3759	0.33	0.19
	60	0.0128	0.0602	0.7162	0.33	0.22

_____
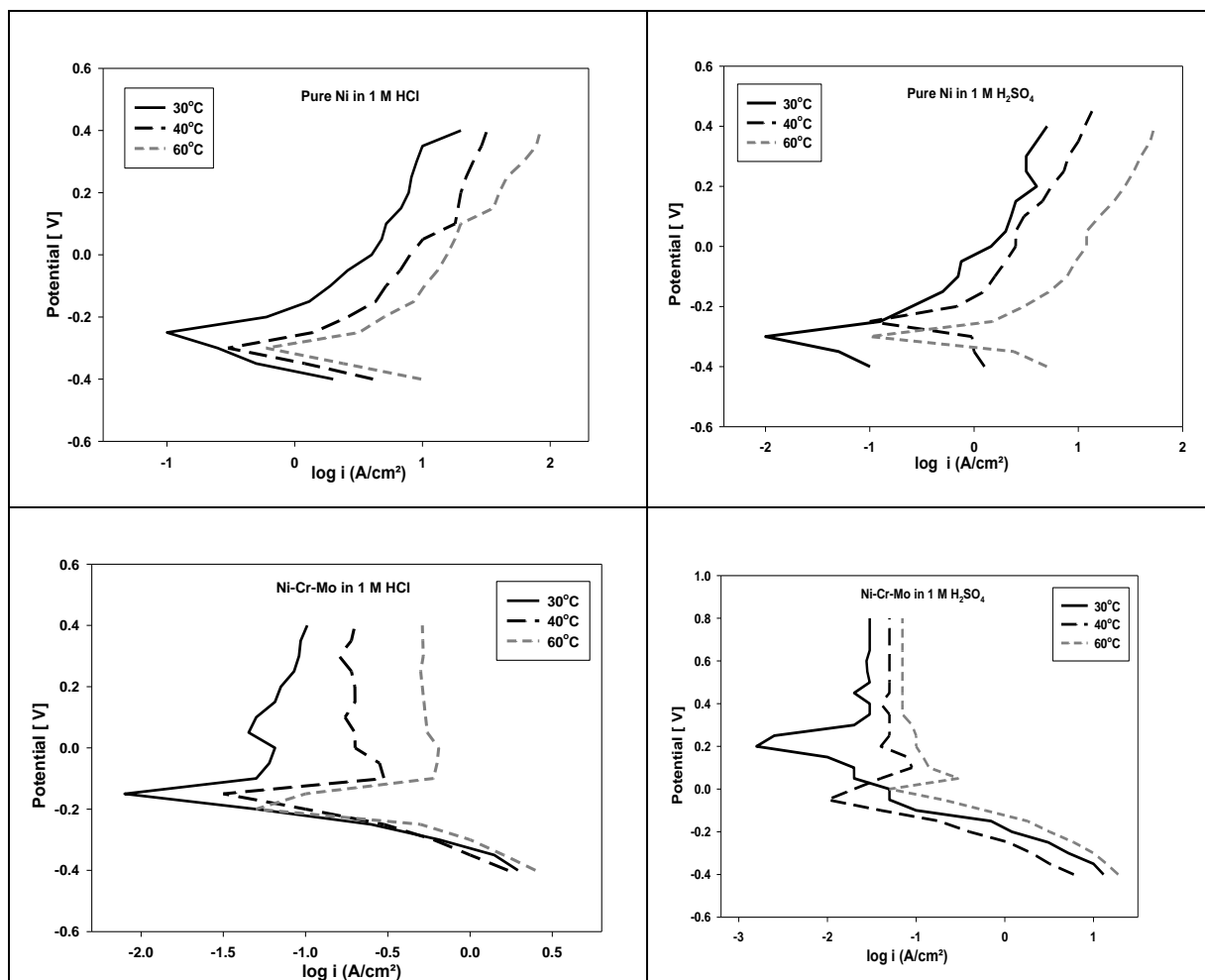
Fig. 4. Potentiodynamic polarization curves of pure Ni and 65Ni-24Cr-10Mo alloy in acidic media at different acidic media and temperatures

Kinetic and thermodynamic parameters are also calculated from the results of the corrosion rate by potentiodynamic measurements. The ln (C.R.) vs. absolute temperature (1/T) reciprocal plot as shown in Fig. 5. It provides a straight line with slope= $-$ Ea / R from which the values of the activation energy for the corrosion process are measured and tabulated in Table 3. A plot of ln (CR/T) vs. 1/T which illustrates in Fig. 6. exists a straight show with slope = $-\Delta H_{ands}$ /R and intercept = ln(R/Nh) + ΔS_{ads} /R. The calculated values of enthalpy and entropy from the plots are presented in Table 3. The values of the entropy change (ΔS) for the corrosion of 65Ni-24Cr-10Mo alloy in HCl and H_2SO_4 acids are -20.345, -88.264 J/(mol.K) and for pure Ni

are -43.216, -147.83 J/(mol.K). The positive values of $\Delta H°$ reflected the endothermic nature of the dissolution process. Finally, it can be observed that in all acid used, the 65Ni-24Cr-10Mo alloy has higher corrosion resistance than pure Ni. The Cr impact in the presence of oxygen, it enhances the formation of passive surface films. Such passive films inhibit the process of corrosion. It provides extended protection by forming protective oxides. Also, the H_2SO_4 solution is an oxidizing atmosphere which encourages containing a passive layer and decreasing the corrosion rate, but the HCl solution to promote the breakdown of the passive layer.

_____

Table 3. The values of activation parameters of pure Ni and 65Ni-24Cr-10Mo alloy in different acids media from corrosion rate values by potentiodynamic polarization method

Samples	HCl			H$_2$SO$_4$		
	E_a kJ/mole	ΔH kJ/mole	ΔS J/(mole.K)	E_a kJ/mole	ΔH kJ/mole	ΔS J/(mole.K)
Pure Ni	77.157	74.515	-43.216	33.452	30.805	-147.83
65Ni-24Cr-10Mo alloy	72.878	70.232	-20.345	55.574	52.930	-88.264

(a)   (b)
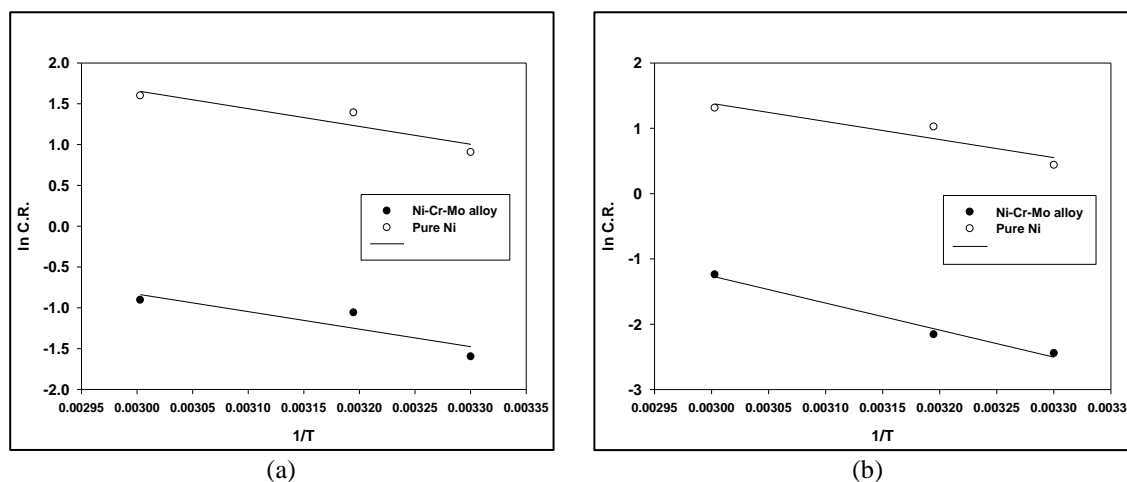
Fig. 5. Arrhenius plots of ln C.R. vs. 1/T for pure Ni and 65Ni-24Cr-10Mo alloy by potentiodynamic polarization method exposed to different acids solutions (a) 1 M HCl and (b) 1M H$_2$SO$_4$

(a)   (b)
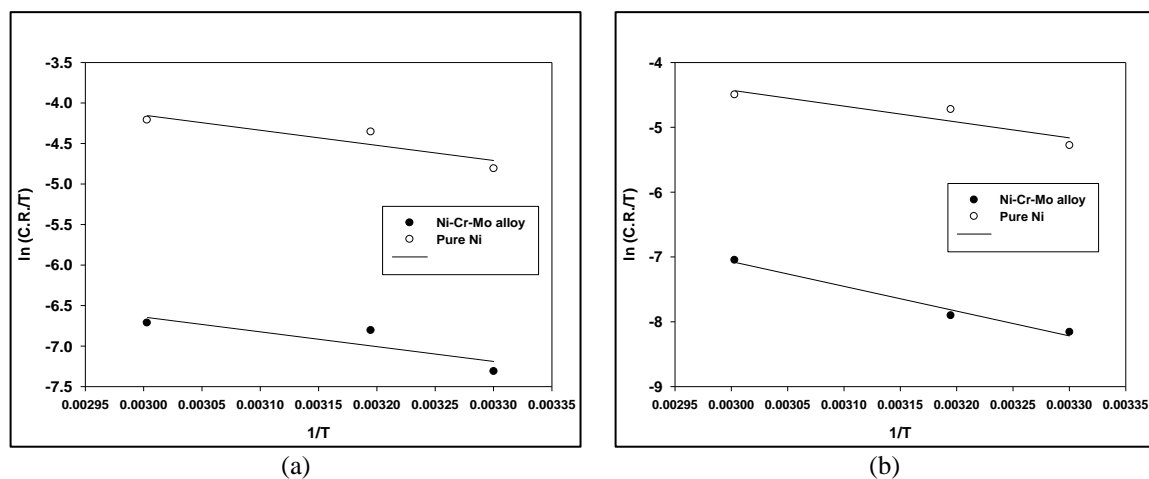
Fig. 6. Plots of ln (C.R./T) versus 1/T for pure Ni and 65Ni-24Cr-10Mo alloy by potentiodynamic polarization method exposed to different acids solutions (a) 1 M HCl and (b) 1M H$_2$SO$_4$

3.3. Surface Morphology

After its long immersion time exposure in the acid test solution (96 hrs), the SEM / EDAX was examined to see the surface morphology and the elemental analysis of the components on the alloy surfaces. Fig. 7. displays SEM micrographs for pure Ni and 65Ni-24Cr-10Mo alloy surfaces after immersion in 1 M HCl solution, which is the higher corrosion rate, for 96 hr and the corresponding EDAX profile analysis as shown in the SEM image. The surface morphology results in HCl acid solution after 96 hr showed that a thick layer of corrosion products in pure Ni than on the 65Ni-24Cr-10Mo alloy. The EDAX analysis of the

corroded pure Ni has 26.5%O, 6.0%Cl and 67.5%Ni as illustrated in Fig. 7(a), and the EDAX result of the 65Ni-24Cr-10Mo alloys is 9.7%O, 2.7%Cl, 24.1%Cr, 50.5%Ni and 12.2%Mo as seen in Fig. 7(b). The oxygen content in the EDAX analysis may be due to expose the corroded samples to the air. With a thin layer of corrosion products with some deposits, the pure Ni surface looks smooth and homogeneous. Therefore, due to the corrosive assault of the acid solution on its surface, the alloy suffers uniform corrosion and there is no evidence of localized corrosion. The existence of oxygen indicates that the layer of the corrosion product may contain certain oxides such as NiO, Cr_2O_3, and MoO_2, which may protect the alloy surface [12]. NiO, which is not as stable as the Cr oxides and the spinel phases [25], may have been stimulated by the additional Ni. The representation of SEM is shown in Fig. 7. The 65Ni-24Cr-10Mo alloy surface displays a thicker product layer of corrosion relative to pure Ni corrosion products. The elements found on the surface of the alloy as shown in Fig. 7 and depicted in the same Figure by the EDAX pattern. There, because of the

formation of thick layers of corrosion materials, the very small concentrations of Ni, Cr and Mo relative to their values in the alloy before their exposure to the acid solution. The high percentage of oxygen detected suggested that the layer formed on the surface of the alloy has some films of oxide. The presence of these oxides would increase the alloy's passivity as its corrosion resistance to the tough result of the acid solution to the alloy surface. Therefore, it is assumed that the formed layer of corrosion products that cover the entire alloy surface and decrease the acid molecules' aggressive attack on it and confirms the data obtained by the method of weight-loss and potentiodynamic measurements. In pure Ni containing dissolved oxygen is 21.9 % or under oxidizing conditions, were corroded seriously due to oxygen diffusion through the porous oxide layer consisting of ~-$Ni(OH)_2$. On the other hand, 65Ni-24Cr-10Mo alloy was resistant to corrosion because Ni was involved in H_2 oxidation in the alloys. The specimens were corroded at high temperatures by de-aerated solution in which the evolution of H_2 occurred as the counter-reaction [17].
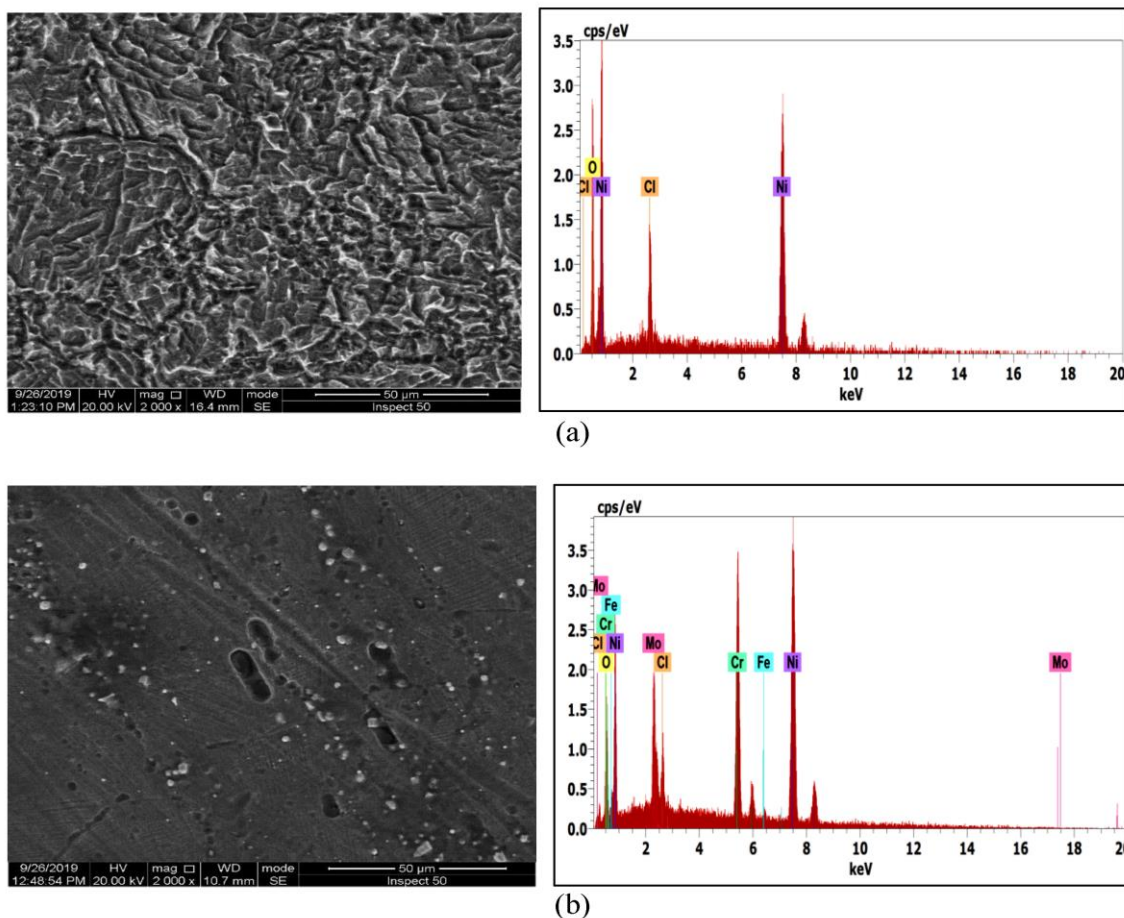

Fig. 7. SEM/ EDAX micrographs after its immersion in 1M HCl solutions for 96 hr
(a) pure Ni and (b) 65Ni-24Cr-10Mo alloy

4. Conclusion

The corrosion behavior of pure Ni and 65Ni-24Cr-10Mo alloy was investigated in HCl and H_2SO_4 acidic solutions and different temperatures. The effect of temperature at a constant concentration of acid as in the case of 1 M HCl solution has a strong influence on the rate of corrosion of pure Ni, but the corrosion rate of the 65Ni-24Cr-10Mo alloy is almost unaffected by low activation energy. The corrosion rates of the 65Ni-24Cr-10Mo alloy are higher than for pure Ni in different acidic media. The 65Ni-24Cr-10Mo alloy has a good corrosion resistance than pure Ni in different acidic media due to the existence of Cr and Mo. The corrosion rate of the 65Ni-24Cr-10Mo alloy in HCl solution is more than in H_2SO_4 solution. The H_2SO_4 solution is an oxidizing atmosphere which encourages containing a passive layer and decrease the corrosion rate but the HCl solution promote to break down of the passive layer. The surface morphology results for the higher corrosion rate media (HCl acid solution after 96 hr) showed that a thick layer of corrosion products in pure Ni than on the 65Ni-24Cr-10Mo alloy.

5. Conflicts of interest

There are no conflicts to declare.

6. References

[1]. Y. Reda, K. M. Zohdy, A. K. Eessaa, A. M. El-Shamy, Effect of Plating Materials on the Corrosion Properties of Steel Alloy 4130, Egypt. J. Chem., 63 (2): 579–597 (2020).

[2]. Y. Reda, A. M. El-Shamy, K. M. Zohdy, A. K. Eessaa, Instrument of chloride ions on the pitting corrosion of electroplated steel alloy 4130, Ain Shams Eng. J., 11 (2020) 191–199 (2020).

[3]. Coman V., Robotin B., Ilea P., Nickel recovery/removal from industrial wastes: A review, Resources, Conservation Recycl., 73, 229-238 (2013)

[4]. Klapper H.S., Zadorozne N.S., Rebak R.B., Localized Corrosion Characteristics of Nickel Alloys: A Review, Acta Metall. Sin. (Engl. Lett.), 30(4), 296–305 (2017)

[5]. Abdallah M., Jahdaly B.A.A.AL., Salem M.M., Fawzy A., Mabrouk E.M., Electrochemical Behavior of Nickel Alloys and Stainless Steel in HNO3 using Cyclic Voltammetry Technique, J. Mater. Environ. Sci., 8(4), 1320-1327 (2017)

[6]. Zheng S.Q.,Wang D.N., Qi Y.M., Chen C.F., Chen L.Q., Investigation on the Property Degradation of Nickel-Base Alloy 825 in High Pressure H2S Environments, Int. J. Electrochem. Sci. 7, 12974 (2012)

[7]. Carranza R.M., Rodríguez M.A., Crevice corrosion of nickel-based alloys considered as engineering barriers of geological repositories, Materials Degradation, (2017)

[8]. Svistunova T.V., Runova Z.K., Sakharnov A.A., Knifeline, corrosion of nickel-molybdenum alloys, Metalloved. Term. Obrab. Met., 5, 2-6 (1970)

[9]. Zemskii S.V., Svistunova T.V., Sakuta N.D., Sidorina T.N., Interaction of impurity and alloying elements with grain boundaries in nickel-molybdenum alloys, Metalloved. Term. Obrab. Met., 3, 33 – 34 (1993)

[10]. Svistunova T.V., Sakuta N.D., Lapshina O.B., Effect of cold deformation and aging on the structure and properties of corrosion-resistant Ni – Cr – Mo alloy," Metalloved. Term. Obrab. Met., 1, 14 – 18 (2002)

[11]. Mishra A., Performance of Corrosion-Resistant Alloys in Concentrated Acids, Acta Metall. Sin. (Engl. Lett.), 30(4): 306-318 (2017)

[12]. Svistunova T.V., Corrosion-resistant alloys for very highly corrosive media, Met. Sci. Heat Treat., 47, 7-8, (2005)

[13]. Mohamed L.Z., El Kady O.A., Lotfy M.M., Ahmed H.A., Elrefaie F.A., Characteristics of Ni-Cr binary alloys produced by conventional powder metallurgy, Key Eng. Mater., 835, 214-222 (2020)

[14]. Khandelwal R., Arora S.K., Mathur S.P., Study of plant cordia dichotoma as green Corrosion inhibitor for mild steel in different acid media, E-J. Chem., 3, 1200-1205 (2011)

[15]. Gaber Gh.A., Aly H.A., Mohamed L.Z., Effect of Sodium Tungstate on the Corrosion Behavior of Fe-Base Alloy in H_2SO_4 Solution, Int. J. Electrochem. Sci., 15(8), 8229 – 8240 (2020)

[16]. Afolabi A.S., Muhirwa A. C., Abdulkareem A.S., Muzenda E., Weight loss and microstructural studies of stressed mild steel in apple juice, Int. J. Electrochem. Sci., 9, 5895 – 5906 (2014)

[17]. Kim H., Mitton D.B., Latanision R.M., Effect of pH and temperature on corrosion of nickel-base alloys in high temperature and pressure aqueous solutions, J. Electrochem. Soc., 157 (5), C194-C199 (2010)

[18]. Olasehinde E.F., Olusegu S.J., Adesina A.S., Omogbehin S.A., Yahayah M., Inhibitory action of nicotiana tabacum extracts on the corrosion of mild steel in HCl, J. Natur. Sci., 11(1), 83 – 90 (2013)

[19]. Ahmad M., Al-haj A., Nabeel A., D. Nuhu, Rihan O., Thermodynamics and kinetics of inhibition of aluminum in hydrochloric acid by date palm leaf

extract, J. Appl. Sci. Envir., 18, 3, 543 – 551, (2014)

[20]. Ghanem W.A., Ahmed A.S.I., Hussein W.A., Gaber Gh.A., Electrochemical behavior and effect of temperature on dezincification of Cu-Zn alloys in brine solutions, Inter. J Metallurg. Mater. Sci. Eng., 6(4), 1-16(2016)

[21]. Gaber Gh.A., Maamoun M.A., Ghanem W.A., Evaluation of the inhibition efficiency of a green inhibitor on corrosion of Cu-Ni alloys in the marine application, Key Eng. Mater., 786, 174-194 (2018)

[22]. Rania H. Taha, Ghalia A. Gaber, Lamiaa Z. Mohamed, Wafaa A. Ghanem, Corrosion Inhibition of Two Schiff Base Complexes on The Mild Steel in 1M HCl Solution, Egypt. J. Chem. 62(Special Issue (Part 1)), 367 - 381 (2019)

[23]. Go L.C., Depan D., Holmes W.E., Gallo A., Knierim K., Bertrand T., Hernandez R., Kinetic and thermodynamic analyses of the corrosion inhibition of synthetic extracellular polymeric substances, Peer J Materials Science, (2020)

[24]. Gaber Gh.A., Maamoun M.A., Ghanem W.A., Evaluation of the inhibition efficiency of a green inhibitor on corrosion of Cu-Ni alloys in the marine application, Key Eng. Mater., 786, 174-194 (2018)

[25]. Tan L., Ren X., Sridharan K., Allen T.R., Corrosion behavior of Ni-base alloys for advanced high temperature water-cooled nuclear plants, Corros. Sci., 50, 3056–3062 (2008)